

BOUNDARY CONDITIONS OF THE RGE FLOW IN NONCOMMUTATIVE COSMOLOGY

DANIEL KOLODRUBETZ AND MATILDE MARCOLLI

ABSTRACT. We investigate the effect of varying boundary conditions on the renormalization group flow in a noncommutative geometry model. Specifically, changing conditions at unification energy run down to the electroweak scale. Varying a value even slightly can be shown to have drastic effects on the running of many model parameters. The model used has several constraints at the unification scale. These restrictions arise out of the geometry of the model. Matching these constraint and adjusting other parameters, it is possible to get the renormalization flow to agree in order of magnitude with the predictions at the electroweak scale.

CONTENTS

1. Introduction	1
2. The spectral action and the renormalization group flow	3
2.1. The asymptotic form of the spectral action	3
2.2. Renormalization group flow	5
3. Effects of changing boundary conditions	6
3.1. The default boundary conditions	6
3.2. Maximal mixing example	7
3.3. Running coefficients with changing boundary conditions	8
4. Geometric constraints at unification	9
4.1. Constraint on λ	9
4.2. The α parameter and the Higgs vacuum	9
4.3. Constraint on c	9
4.4. The mass relation at unification	10
5. Low energy physical constraints	11
5.1. Boundary conditions at the electroweak scale	11
5.2. Comparison of expected and measured values	11
References	12

1. INTRODUCTION

The recent work [5] developed cosmological models of the very early universe based on the particle physics model of [3] derived from noncommutative geometry, via the formalism of spectral triple and the spectral action

functional. In these particle physics models, the Lagrangian is obtained by computing the asymptotic expansion at high energy of the spectral action functional on a noncommutative space which is the product of an ordinary (commutative) spacetime manifold and extra dimensions given in the form of a noncommutative space which is metrically zero-dimensional, but K-theoretically six dimensional. The choice of the noncommutative space determines the particle physics content of the model and the gauge symmetries. The masses and mixing angles arise geometrically as coordinates on the moduli space of Dirac operators of the spectral triple describing the extra dimensions. In the case of the model developed in [3], the particle physics content is the same as in the ν MSM, namely, in addition to the particles of the Minimal Standard Model, one has right handed neutrinos with Majorana mass terms. However, the model is significantly different from ν MSM when it comes to the properties of the action functional. In fact, as proved in [3], the asymptotic expansion of the spectral action contains the full Standard Model Lagrangian, with the additional Majorana terms for the right handed neutrinos. One has unification of the coupling constants of the three forces, hence the model has a preferred energy scale at unification. The asymptotic expansion of the spectral action also contains gravitational terms, which are the most interesting part from the point of view of applications to cosmological models. These terms contain an Einstein–Hilbert term, a cosmological term, a conformal gravity term, a non-dynamical topological term, and a conformal coupling of the Higgs field to gravity. Moreover, the usual gravitational and cosmological constants are replaced in this model by effective constants, which run with the energy scale, through their dependence on the Yukawa parameters of the particle physics content of the model. In [5] the resulting running of effective gravitational and cosmological constants is analyzed and several consequences on early universe cosmology are obtained, from mechanisms for inflation to effects on the gravitational waves and the evaporation law for primordial black holes. The analysis performed in [5] depends on the choice of initial boundary conditions at unification for the renormalization group flow. The results of [5] are obtained using the default boundary conditions of [1]. However, as we show in the present paper, one obtains significantly different behaviors of the coefficients of the asymptotic expansion of the spectral action by changing boundary conditions. This implies that there will be the possibility of drawing interesting exclusion curves in the space of all possible boundary conditions, on the basis of comparing the model with cosmological data, for example through the predictions for the tensor-to-scalar ratio and the spectral index derived in [5]. For the purpose of the present paper, we first show how one obtains significantly different curves for the running of the parameters in the action functional with different choices of the boundary conditions. Then we give examples of boundary conditions that match the geometric constraints at unification derived in [3], and then we estimate, in these examples, the discrepancy with respect to the physical prediction at low energy. An important aspect

of these models is understanding how much nonperturbative effects in the spectral action may affect the low energy behavior of the model, since that is the main obstacle to extending to the more recent universe the cosmological models of [5]. Our estimates of the low energy behavior when matching geometric boundary conditions at unification may also provide some indirect evidence for the magnitude of such effects.

2. THE SPECTRAL ACTION AND THE RENORMALIZATION GROUP FLOW

In noncommutative geometry one models the analog of a Riemannian manifold through the notion of a *spectral triple*, consisting of data $(\mathcal{A}, \mathcal{H}, \mathcal{D})$ of an involutive algebra, a Hilbert space representation, and a Dirac operator, which has the compatibility condition of having bounded commutators with elements of the algebra. Additional structure, in the form of grading γ and real involution J with compatibility conditions with the data $(\mathcal{A}, \mathcal{H}, \mathcal{D})$ are also introduced. In the particle physics context, γ corresponds to the two chiralities of fermions and J to the involution that exchanges particles and antiparticles. See [3] for a more detailed account of the underlying mathematical structure, which we do not recall here. The action functional considered in noncommutative geometry models for particle physics is based on the spectral action [2] for the Dirac operator of a spectral triple, with additional fermionic terms. In the model of [3] this takes the form

$$(2.1) \quad \text{Tr}(f(D_A/\Lambda)) + \frac{1}{2} \langle J\tilde{\xi}, D_A\tilde{\xi} \rangle.$$

Here $D_A = D + A + \varepsilon' J A J^{-1}$ is the Dirac operator with inner fluctuations given by the gauge potentials of the form $A = A^\dagger = \sum_k a_k [D, b_k]$, for elements $a_k, b_k \in \mathcal{A}$. The ε' is just a function of $n \bmod 8$ that gives -1 for n congruent to $1 \bmod 4$ and 1 for all other values of n . The fermionic term $\langle J\tilde{\xi}, D_A\tilde{\xi} \rangle$ should be seen as a pairing of classical fields $\tilde{\xi} \in \mathcal{H}^+ = \{\xi \in \mathcal{H} \mid \gamma\xi = \xi\}$, viewed as Grassmann variables. For the purpose of cosmological applications, the most important part of this action functional is the one that comes from the asymptotic expansion at high energy Λ of the spectral action $\text{Tr}(f(D_A/\Lambda))$, since this contains the gravitational terms and their coupling to matter.

2.1. The asymptotic form of the spectral action. The asymptotic expansion of the spectral action is obtained in the form (see [2], [3])

$$(2.2) \quad \text{Tr}(f(D/\Lambda)) \sim \sum_{k \in \text{DimSp}^+} f_k \Lambda^k \int |D|^{-k} + f(0) \zeta_D(0) + o(1),$$

where $f_k = \int_0^\infty f(v) v^{k-1} dv$ are the momenta of the function f and the noncommutative integration is defined in terms of residues of zeta functions

$$(2.3) \quad \zeta_{a,D}(s) = \text{Tr}(a |D|^{-s}).$$

The sum in (2.2) is over points in the *dimension spectrum* of the spectral triple, which is a refined notion of dimension for noncommutative spaces,

consisting of the set of poles of the zeta functions (2.3). More explicitly, as proved in [3], when applied to a noncommutative space of the form $X \times F$, with X an ordinary 4-dimensional (Euclidean) spacetime and F the non-commutative space whose algebra of coordinates is $\mathbb{C} \oplus \mathbb{H} \oplus M_3(\mathbb{C})$, with \mathbb{H} the algebra of quaternions, the expansion (2.2) of $\text{Tr}(f(D_A/\Lambda))$ gives terms of the form

$$\begin{aligned}
 S = & \frac{1}{2\kappa_0^2} \int R \sqrt{g} d^4x + \gamma_0 \int \sqrt{g} d^4x \\
 & + \alpha_0 \int C_{\mu\nu\rho\sigma} C^{\mu\nu\rho\sigma} \sqrt{g} d^4x + \tau_0 \int R^* R^* \sqrt{g} d^4x \\
 (2.4) \quad & + \frac{1}{2} \int |DH|^2 \sqrt{g} d^4x - \mu_0^2 \int |H|^2 \sqrt{g} d^4x \\
 & - \xi_0 \int R |H|^2 \sqrt{g} d^4x + \lambda_0 \int |H|^4 \sqrt{g} d^4x \\
 & + \frac{1}{4} \int (G_{\mu\nu}^i G^{\mu\nu i} + F_{\mu\nu}^\alpha F^{\mu\nu\alpha} + B_{\mu\nu} B^{\mu\nu}) \sqrt{g} d^4x.
 \end{aligned}$$

The coefficients of these terms are functions

$$\begin{aligned}
 \frac{1}{2\kappa_0^2} &= \frac{96f_2\Lambda^2 - f_0\mathfrak{c}}{24\pi^2} \\
 \gamma_0 &= \frac{1}{\pi^2} (48f_4\Lambda^4 - f_2\Lambda^2\mathfrak{c} + \frac{f_0}{4}\mathfrak{d}) \\
 \alpha_0 &= -\frac{3f_0}{10\pi^2} \\
 (2.5) \quad \tau_0 &= \frac{11f_0}{60\pi^2} \\
 \mu_0^2 &= 2\frac{f_2\Lambda^2}{f_0} - \frac{\mathfrak{e}}{\mathfrak{a}} \\
 \xi_0 &= \frac{1}{12} \\
 \lambda_0 &= \frac{\pi^2\mathfrak{b}}{2f_0\mathfrak{a}^2}.
 \end{aligned}$$

These depend upon the three parameters f_0 , f_2 , f_4 , where $f_0 = f(0)$ and for $k > 0$

$$f_k = \int_0^\infty f(v) v^{k-1} dv,$$

where f_0 depends upon the common value of the coupling constants at unification energy and f_2 and f_4 are free parameters of the model. The expressions (2.5) also depend upon the energy scale Λ and the running of these parameters is the main topic of our present investigation. In addition to the explicit dependence on Λ of the coefficients (2.5) there is also an additional and very interesting dependence on Λ through the coefficients \mathfrak{a} , \mathfrak{b} , \mathfrak{c} , \mathfrak{d} and \mathfrak{e} . These are functions of the Yukawa parameters and Majorana masses of

the particle physics content of the model, in the form

$$\begin{aligned}
 \mathfrak{a} &= \text{Tr}(Y_\nu^\dagger Y_\nu + Y_e^\dagger Y_e + 3(Y_u^\dagger Y_u + Y_d^\dagger Y_d)) \\
 \mathfrak{b} &= \text{Tr}((Y_\nu^\dagger Y_\nu)^2 + (Y_e^\dagger Y_e)^2 + 3(Y_u^\dagger Y_u)^2 + 3(Y_d^\dagger Y_d)^2) \\
 (2.6) \quad \mathfrak{c} &= \text{Tr}(MM^\dagger) \\
 \mathfrak{d} &= \text{Tr}((MM^\dagger)^2) \\
 \mathfrak{e} &= \text{Tr}(MM^\dagger Y_\nu^\dagger Y_\nu).
 \end{aligned}$$

2.2. Renormalization group flow. We use, as in [5] the renormalization group equations for the Standard Model with right handed neutrinos and Majorana mass terms of [1]. The numerical results described here are obtained with a Mathematica code based on the REAP program of [1] adapted to our model by the first author.

We recall here that the RGE for this particle physics model is given (at one loop) by the beta functions

$$\begin{aligned}
 16\pi^2 \beta_{g_i} &= b_i g_i^3 \quad \text{with } (b_{SU(3)}, b_{SU(2)}, b_{U(1)}) = (-7, -\frac{19}{6}, \frac{41}{10}) \\
 16\pi^2 \beta_{Y_u} &= Y_u(\frac{3}{2}Y_u^\dagger Y_u - \frac{3}{2}Y_d^\dagger Y_d + \mathfrak{a} - \frac{17}{20}g_1^2 - \frac{9}{4}g_2^2 - 8g_3^2) \\
 16\pi^2 \beta_{Y_d} &= Y_d(\frac{3}{2}Y_d^\dagger Y_d - \frac{3}{2}Y_u^\dagger Y_u + \mathfrak{a} - \frac{1}{4}g_1^2 - \frac{9}{4}g_2^2 - 8g_3^2) \\
 16\pi^2 \beta_{Y_\nu} &= Y_\nu(\frac{3}{2}Y_\nu^\dagger Y_\nu - \frac{3}{2}Y_e^\dagger Y_e + \mathfrak{a} - \frac{9}{20}g_1^2 - \frac{9}{4}g_2^2) \\
 16\pi^2 \beta_{Y_e} &= Y_e(\frac{3}{2}Y_e^\dagger Y_e - \frac{3}{2}Y_\nu^\dagger Y_\nu + \mathfrak{a} - \frac{9}{4}g_1^2 - \frac{9}{4}g_2^2) \\
 16\pi^2 \beta_M &= Y_\nu Y_\nu^\dagger M + M(Y_\nu Y_\nu^\dagger)^T \\
 16\pi^2 \beta_\lambda &= 6\lambda^2 - 3\lambda(3g_2^2 + \frac{3}{5}g_1^2) + 3g_2^4 + \frac{3}{2}(\frac{3}{5}g_1^2 + g_2^2)^2 + 4\lambda\mathfrak{a} - 8\mathfrak{b}
 \end{aligned}$$

Notice that we use here the normalization of the coupling constants used in [1], which is different from the one of [3].

In particular, as in [1], we solve numerically these equations using different effective field theories in the intervals of energies between the three see-saw scales, with matching boundary conditions. Namely, starting from assigned boundary conditions at unification, one runs the RGE flow down until the first see-saw scale (the top eigenvalue of the Majorana mass matrix M). Then one integrates out the higher modes by introducing a first effective theory with Yukawa parameters $Y_\nu^{(3)}$ obtained by removing the last row of Y_ν in the basis where M is diagonal and with Majorana mass matrix $M^{(3)}$ obtained by removing the last row and column. One then restarts the RGE flow for these new variables with matching boundary conditions at the top see-saw scale, until the second see-saw scale, and so on. One has in this way effective field theories $(Y_\nu^{(k)}, M^{(k)})$, $k = 3, 2, 1$.

We study the effect on this RGE flow of changing boundary conditions at unification scale, and we then derive consequences for the running of the coefficients $\mathfrak{a}, \mathfrak{b}, \mathfrak{c}, \mathfrak{d}, \mathfrak{e}$ in the asymptotic expansion of the spectral action.

3. EFFECTS OF CHANGING BOUNDARY CONDITIONS

The REAP program from [1] allows the user to adjust the boundary conditions. These changes are generally made at Λ_{unif} , taken here to be 2×10^{16} GeV. As we understand that only fine tuned initial conditions for the universe allowed its current form, we expect the boundary conditions at unification energy to drastically effect the development of our model parameters.

3.1. The default boundary conditions. The boundary conditions at unification used in [5] are the default boundary conditions of [1]. These have the following values.

$$\lambda(\Lambda_{unif}) = \frac{1}{2}$$

$$Y_u(\Lambda_{unif}) = \begin{pmatrix} 5.40391 \times 10^{-6} & 0 & 0 \\ 0 & 0.00156368 & 0 \\ 0 & 0 & 0.482902 \end{pmatrix}$$

For $Y_d(\Lambda_{unif}) = (y_{ij})$ they have

$$\begin{aligned} y_{11} &= 0.0000482105 - 3.382 \times 10^{-15}i \\ y_{12} &= 0.000104035 + 2.55017 \times 10^{-7}i \\ y_{13} &= 0.0000556766 + 6.72508 \times 10^{-6}i \\ y_{21} &= 0.000104035 - 2.55017 \times 10^{-7}i \\ y_{22} &= 0.000509279 + 3.38205 \times 10^{-15}i \\ y_{23} &= 0.00066992 - 4.91159 \times 10^{-8}i \\ y_{31} &= 0.000048644 - 5.87562 \times 10^{-6}i \\ y_{32} &= 0.000585302 + 4.29122 \times 10^{-8}i \\ y_{33} &= 0.0159991 - 4.21364 \times 10^{-20}i \end{aligned}$$

$$Y_e(\Lambda_{unif}) = \begin{pmatrix} 2.83697 \times 10^{-6} & 0 & 0 \\ 0 & 0.000598755 & 0 \\ 0 & 0 & 0.0101789 \end{pmatrix}$$

$$Y_{nu}(\Lambda_{unif}) = \begin{pmatrix} 1 & 0 & 0 \\ 0 & 0.5 & 0 \\ 0 & 0 & 0.1 \end{pmatrix}$$

$$M(\Lambda_{unif}) = \begin{pmatrix} -6.01345 \times 10^{14} & 3.17771 \times 10^{12} & -6.35541 \times 10^{11} \\ 3.17771 \times 10^{12} & -1.16045 \times 10^{14} & 5.99027 \times 10^{12} \\ -6.35541 \times 10^{11} & 5.99027 \times 10^{12} & -4.6418 \times 10^{12} \end{pmatrix}$$

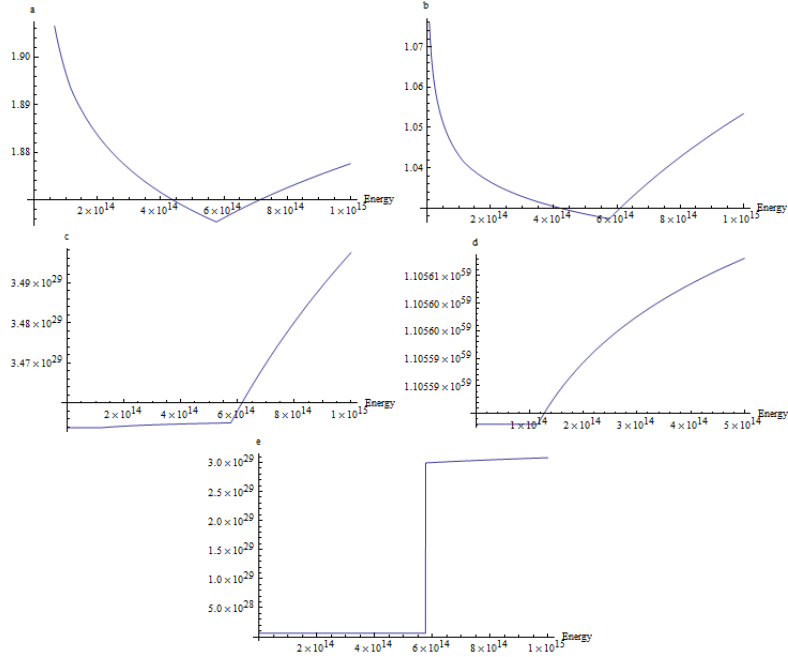


Figure 1. The running coefficients with default boundary conditions near top see-saw scale

3.2. Maximal mixing example. To look at the maximal mixing case, we simply change Y_{nu} at unification energy. With maximal mixing, our parameters will take these values.

$$\zeta = \exp(2\pi i/3)$$

$$U_{PMNS}(\Lambda_{unif}) = \frac{1}{3} \begin{pmatrix} 1 & \zeta & \zeta^2 \\ \zeta & 1 & \zeta \\ \zeta^2 & \zeta & 1 \end{pmatrix}$$

From the available estimates of the neutrino masses, we get the diagonal mass matrix

$$\delta_{(\uparrow 1)} = \frac{1}{246} \begin{pmatrix} 12.2 \times 10^{-9} & 0 & 0 \\ 0 & 170 \times 10^{-6} & 0 \\ 0 & 0 & 15.5 \times 10^{-3} \end{pmatrix}$$

Finally,

$$Y_{nu} = U_{PMNS}^\dagger \delta_{(\uparrow 1)} U_{PMNS}$$

Using this form for Y_{nu} and the default boundary conditions all other parameters, we can look at the running coefficients. From the figures below, we see that there are vast differences in the development of the parameters with this boundary condition change.

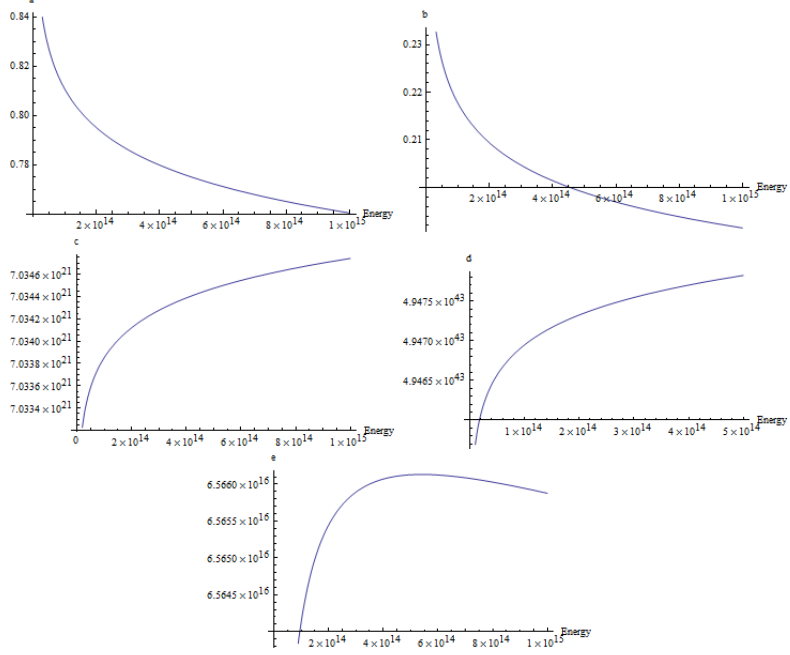


Figure 2. The running coefficients with maximal mixing boundary conditions near top see-saw scale

3.3. Running coefficients with changing boundary conditions. It is possible to get even more interesting behavior by using less standard boundary conditions. By changing just one parameter we can examine how it affects the flow of our running parameters. A specific example is the Y_{nu} matrix. Using our standard boundary conditions, this matrix is diagonal at unification energy. We can adjust each of these elements on the diagonal, which correspond to our neutrino masses, to affect our flow. Using animation functions in Mathematica, it is possible to get a nearly continuous idea of how the flow of our parameters develops with our boundary conditions. The figures below illustrate such a development discretely.

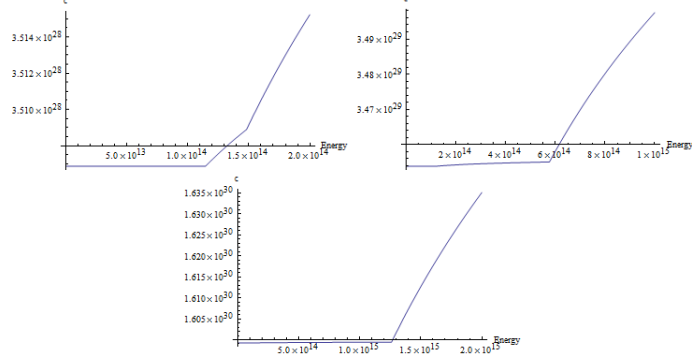


Figure 2. Coefficient c at the upper see-saw scale with the first term of Y_{nu} as 0.5, 1.0, and 1.5 respectively

In these diagrams, we notice the transition changing as the upper neutrino mass varies. The sharp transition at the upper see-saw scale comes from the program integrating out the heavy neutrino at this scale. The second plot shows the behavior we expect from the standard conditions. In the first plot we can see the upper and middle transitions are much closer together than in our second plot. The final plot shows the transition at a much higher energy, corresponding to the higher neutrino mass. From these and other such plots, we learn how the running develops independently by changing different parameters. Of course, changing multiple parameters complicates this development and is dealt with in more detail when matching specific boundary conditions.

4. GEOMETRIC CONSTRAINTS AT UNIFICATION

There are some constraints on the boundary conditions at unification that are imposed by the underlying geometry of the model. These are derived in [3], see also the discussion in §1 of [4]. We recall them here. Not all of these constraints are satisfied by the default boundary conditions of [1], so a first improvement on the model of [5] is to identify choices of boundary conditions that satisfy these constraints, and then, among them, eliminate those that produce non-physical predictions.

4.1. Constraint on λ . A first constraint imposed by the geometry is on the value of the Higgs self-coupling λ at unification. This satisfies

$$(4.1) \quad \lambda(\Lambda_{unif}) = \frac{\pi^2}{2f_0} \frac{\mathfrak{b}(\Lambda_{unif})}{\mathfrak{a}(\Lambda_{unif})^2}.$$

Looking at our maximal mixing boundary conditions we can calculate that $\lambda(\Lambda_{unif}) = 2.989$. By setting it to this value at unification energy in our flow we can ensure that this requirement is met.

4.2. The \mathfrak{a} parameter and the Higgs vacuum. The model of [3] also relates the parameter \mathfrak{a} to the Higgs vacuum through the relation

$$(4.2) \quad \frac{\sqrt{\mathfrak{a}f_0}}{\pi} = \frac{2M_W}{g},$$

where g is the common value of the coupling constants at unification and M_W is the W -boson mass. As M_W is directly proportional to $\sqrt{\mathfrak{a}}$, this condition is a statement of the equality of f_0 and the coupling constants at unification energy.

4.3. Constraint on \mathfrak{c} . The see-saw mechanism is implemented in [3] geometrically, through the fact that the restriction of the Dirac operator $D(Y)$

to the subspace of \mathcal{H}_F spanned by $\nu_R, \nu_L, \bar{\nu}_R, \bar{\nu}_L$ is of the form

$$(4.3) \quad \begin{pmatrix} 0 & M_\nu^\dagger & \bar{M}_R^\dagger & 0 \\ M_\nu & 0 & 0 & 0 \\ \bar{M}_R & 0 & 0 & \bar{M}_\nu^\dagger \\ 0 & 0 & \bar{M}_\nu & 0 \end{pmatrix},$$

where M_ν is the neutrino mass matrix, see Lemma 1.225 of [4]. This imposes a constraint at unification on the coefficient \mathfrak{c} , of the form

$$(4.4) \quad \frac{2f_2\Lambda_{unif}^2}{f_0} \leq \mathfrak{c}(\Lambda_{unif}) \leq \frac{6f_2\Lambda_{unif}^2}{f_0}.$$

By setting our Majorana mass matrix to 10 times its default value, the inequality can be matched. In this particular case, the f_2 that is used is in the range given in [5]. f_0 is calculated from the coupling constants at unification energy.

4.4. The mass relation at unification. Another prediction which is specific to the model of [3] is a quadratic relation between the masses at unification scale, of the form

$$(4.5) \quad \sum_{generations} (m_\nu^2 + m_e^2 + 3m_u^2 + 3m_d^2)|_{\Lambda=\Lambda_{unif}} = 8M_W^2|_{\Lambda=\Lambda_{unif}},$$

where m_ν, m_e, m_u , and m_d are the masses of the leptons and quarks, that is, the eigenvectors of the matrices $\delta_{\uparrow 1}, \delta_{\downarrow 1}, \delta_{\uparrow 3}$ and $\delta_{\downarrow 3}$, respectively, and M_W is the W-boson mass. We use the fact that M_W is given as a function of the model parameters by

$$(4.6) \quad \frac{\sqrt{\mathfrak{a}}}{2\sqrt{2}} = M_W.$$

So, our equation becomes

$$(4.7) \quad \sum_{generations} (m_\nu^2 + m_e^2 + 3m_u^2 + 3m_d^2)|_{\Lambda=\Lambda_{unif}} = \mathfrak{a}|_{\Lambda=\Lambda_{unif}}.$$

In our maximal mixing boundary conditions, we get

$$(4.8) \quad \sum_{generations} (m_\nu^2 + m_e^2 + 3m_u^2 + 3m_d^2)|_{\Lambda=\Lambda_{unif}} = 0.6698 = \mathfrak{a}|_{\Lambda=\Lambda_{unif}}.$$

This value of \mathfrak{a} , when converted to conventional units, gives a value of M_W of 72 GeV. The expected value on M_W is around 80 GeV so these boundary conditions are believable. So, by using our maximal mixing boundary conditions with a modified Majorana mass matrix and Higgs parameter, we can meet all of the geometric boundary conditions from the model.

5. LOW ENERGY PHYSICAL CONSTRAINTS

At the electroweak scale, physical data imposes other boundary conditions on some of the Yukawa matrices. Finding the unification scale conditions that can also match these lower energy requirements would be ideal. We look at the conditions that are expected from physical data and compare to the results from the running of the model parameters.

5.1. Boundary conditions at the electroweak scale. Current predictions at the electroweak scale tell us that the CKM matrix at Λ_0 can be taken to be of the form

$$U_{CKM}(\Lambda_0) = \begin{pmatrix} 0.97419 & 0.2257 & 0.00359 \\ 0.2256 & 0.97334 & 0.0415 \\ 0.00874 & 0.0407 & 0.999133 \end{pmatrix}$$

Combined with

$$\delta_{(43)}(\Lambda_0) = \frac{1}{246} \begin{pmatrix} 0.00475 & 0 & 0 \\ 0 & 1 & 0 \\ 0 & 0 & 4.25 \end{pmatrix}$$

we get that the Yukawa parameters for the quarks are given by

$$Y_d = U_{CKM}(\Lambda_0) \delta_{(43)}(\Lambda_0) U_{CKM}(\Lambda_0)^\dagger$$

and

$$Y_u(\Lambda_0) = \frac{1}{246} \begin{pmatrix} 0.0024 & 0 & 0 \\ 0 & 1.25 & 0 \\ 0 & 0 & 173 \end{pmatrix}$$

Similarly, for the matrix of charged leptons, the known values and low energy are

$$Y_e(\Lambda_0) = \frac{1}{246} \begin{pmatrix} 0.000511 & 0 & 0 \\ 0 & 0.1056 & 0 \\ 0 & 0 & 1.777 \end{pmatrix}$$

The conditions for the other parameters are all given at the unification scale.

5.2. Comparison of expected and measured values. We use the modified maximal mixing boundary conditions to run the parameters and compare to the physical boundary conditions at low energy. From this analysis, we get that the measured Yukawa parameters for quarks are

$$Y_{d,measured}(\Lambda_0) = \frac{1}{246} \begin{pmatrix} 0.0121 & 0 & 0 \\ 0 & 0.128 & 0 \\ 0 & 0 & 4.032 \end{pmatrix}$$

and

$$Y_{u,measured}(\Lambda_0) = \frac{1}{246} \begin{pmatrix} 0.0032 & 0 & 0 \\ 0 & 0.9223 & 0 \\ 0 & 0 & 248 \end{pmatrix}$$

For the charged leptons, we get the mass matrix

$$Y_e(\Lambda_0, \text{measured}) = \frac{1}{246} \begin{pmatrix} 0.000699 & 0 & 0 \\ 0 & 0.147 & 0 \\ 0 & 0 & 2.51 \end{pmatrix}$$

Comparing these to the expected values at low energies, we see that the order of magnitude and form of the matrices agree. While the agreement is not exact, it seems that this is the closest we can get while maintaining the geometric constraints of the model. In order to make the agreement more exact, further fine tuning is required.

Acknowledgment. This paper is based on the results of Daniel Kolodrubetz's summer research project supported by Caltech's Summer Undergraduate Research Richter Memorial Fellowship.

REFERENCES

- [1] S. Antusch, J. Kersten, M. Lindner, M. Ratz, M.A. Schmidt *Running neutrino mass parameters in see-saw scenarios*, JHEP 03 (2005) 024, hep-ph/0501272v3.
- [2] A. Chamseddine, A. Connes, *The spectral action principle*. Comm. Math. Phys. 186 (1997), no. 3, 731–750.
- [3] A. Chamseddine, A. Connes, M. Marcolli, *Gravity and the standard model with neutrino mixing*, Adv. Theor. Math. Phys. 11 (2007), no. 6, 991–1089.
- [4] A. Connes, M. Marcolli, *Noncommutative geometry, quantum fields, and motives*. Colloquium Publications, Vol.55, American Mathematical Society, 2008.
- [5] M. Marcolli, E. Pierpaoli, *Early universe models from Noncommutative Geometry*, arXiv:0908.3683

PHYSICS DEPARTMENT, CALIFORNIA INSTITUTE OF TECHNOLOGY, PASADENA, CA 91125, USA

E-mail address: dkolodru@caltech.edu

DEPARTMENT OF MATHEMATICS, CALIFORNIA INSTITUTE OF TECHNOLOGY, PASADENA, CA 91125, USA

E-mail address: matilde@caltech.edu